Supplementary Information (SI) for Materials Advances.

Supplementary information

Zeolitic imidazolate framework decorated bacterial cellulose coating for enhancing particulate filtration and adsorption from liquid and vapour phases of woven fabric

Joanne Li[a], Armando Garcia[b], Anett Kondor[b], Corinne Stone[c], Martin Smith[c], Mike Dennis[c] and Koon-Yang Lee *[a,d]

a. Department of Aeronautics, Imperial College London, South Kensington campus, London, SW7 2AZ, United Kingdom

b. Surface Measurement Systems Ltd., Allentown, PA 18103, United States of America

c. Defence Science and Technology Laboratory, Porton Down, Salisbury, Wiltshire, SP4 0JQ, United Kingdom

d. Institute for Molecular Science and Engineering (IMSE), Imperial College London, SW7 2AZ, United Kingdom

Table of Contents

1. Amount of ZIF-67 decorated on BC

TGA was used to quantify the weight fraction of ZIF-67 in ZIF-BC. The thermal degradation behaviour of neat BC, ZIF-67 and ZIF-BC in N_2 atmosphere is shown in Figure S1. Both BC and ZIF-67 underwent a single step thermal degradation. The onset thermal degradation temperature of BC was found to be 250°C. Beyond this temperature, the cleavage of glycosidic bonds in BC occurred, followed by the partial cross-linking of cellulose molecules leading to the formation of char, as well as the decomposition of cellulose into tar.[5] The onset thermal degradation temperature of ZIF-67 was found to be 500°C. Above this temperature, the 2-MIM ligands decomposed, leading to the collapse of the overall framework structure.[6] A two-step degradation can be seen for ZIF-BC, which corresponded to the thermal degradation of ZIF-67 and BC independently. The residual weight fraction of ZIF-67, neat BC and ZIF-BC at 700°C was found to be 56%, 1% and 35%, respectively. From these values, the ZIF-67 loading on ZIF-BC was estimated to be 62 ± 4 wt.-%.

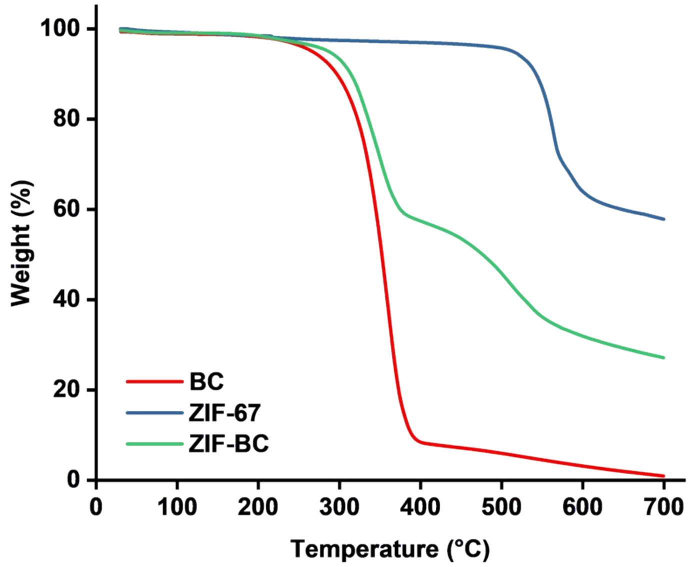

Figure S1. Thermal degradation behavior of BC, ZIF-67 and ZIF-BC.

2. XRD patterns of ZIF-67, BC and ZIF-decorated BC

XRD technique was used to confirm the composition and crystallographic structure of BC, ZIF-67 and ZIF-BC. As shown in Figure S2, the main diffraction peaks observed for BC agree with those reported in literature and are centred around 2θ = 14.5°, 16.5° and 22.5°. The diffraction peak at 2θ = 14.5° corresponds to the diffraction of cellulose Iα(1 0 0) and Iβ(1 $\bar{1}$ 0) reflection planes and the peaks at 2θ = 22.5° corresponds to the diffraction of cellulose Iα(1 1 0) and Iβ(2 0 0) reflection planes.[7] The XRD pattern of the synthesised ZIF-67 matched with the simulated result, with diffraction peaks observed at 2θ = 7.4°, 10.4°, 12.7°, 14.8° and 18.0°. These diffraction peaks correspond to the (0 1 1), (0 0 2), (1 1 2), (0 2 2) and (2 2 2) crystal planes of ZIF-67 respectively [8,9]. It can also be seen from Figure S2 that ZIF-BC has diffraction peaks originated from both BC and ZIF-67, suggesting that ZIF-67 particles were anchored on the surface of BC nanofibrils while maintaining its high crystallinity.

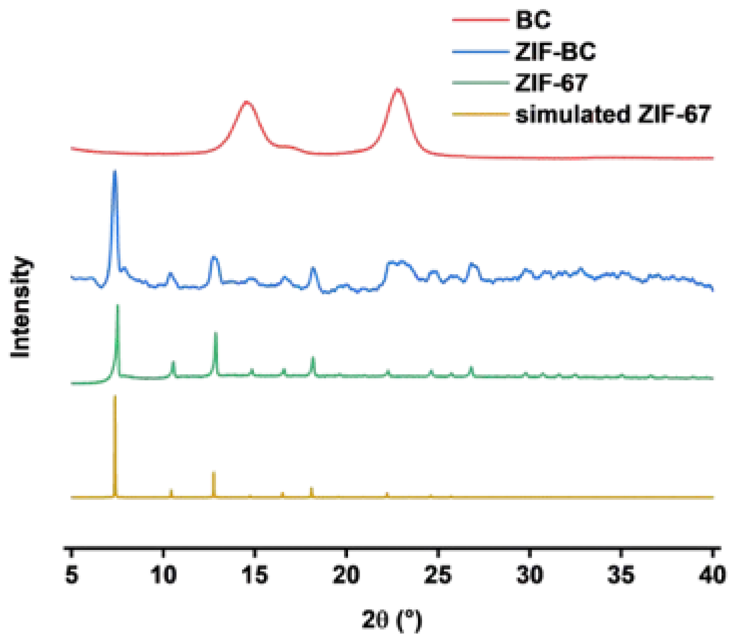

Figure S2. XRD patterns of BC, ZIF-67, ZIF-BC and simulated ZIF-67.

3. ATR-FTIR spectra of ZIF-67, BC and ZIF-decorated BC

To confirm the successful synthesis of ZIF-67 and to elucidate whether ZIF-67 was covalently bonded to BC, ATR-FTIR was conducted (see Figure S3). The ATR-FTIR spectrum of ZIF-67 agrees with those reported in literature. The characteristic absorbance peaks observed for ZIF-67 around ~1570 cm^{-1}, ~1420 cm^{-1}, ~1140 cm^{-1}, ~990 cm^{-1} and 756 cm^{-1} correspond to νN-H,[10] the stretching of the imidazole ring,[11] νC-N,[11, 12] δC-N[12] and the out-of-plane bending of the imidazole ring,[13] respectively. The characteristic absorbance peaks observed for BC at ~3340 cm^{-1}, ~2890 cm^{-1}, ~1420 cm^{-1}, ~1315 cm^{-1}, ~1160 cm^{-1}, ~1110 cm^{-1} and ~1050 cm^{-1} correspond to νOH,[14] νCH,[15] $\delta_s CH_2$,[16] ωCH_2,[17] ν_{as}C-O-C,[16] δOH[18] and δC-O-C,[18] respectively. It can also be seen from Figure 4 that the ATR-FTIR spectrum of ZIF-BC contained the characteristic peaks of both ZIF-67 and BC, corroborating with the fact that the presence of BC nanofibrils did not affect the synthesis of ZIF-67 particles from solution.

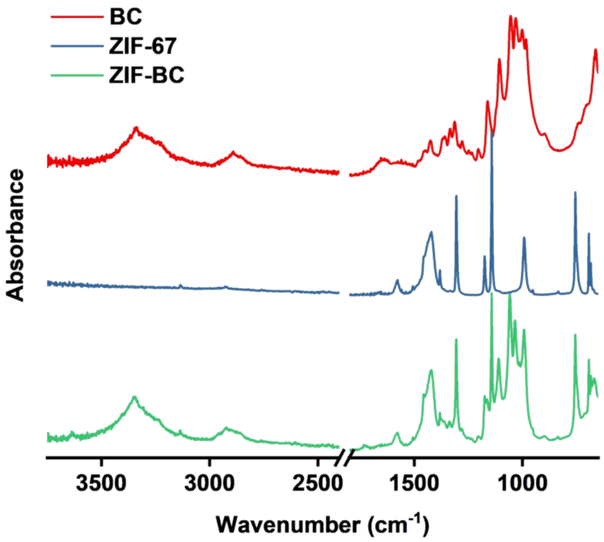

Figure S3. ATR-FTIR spectra of BC, ZIF-67 and ZIF-BC.

4. Congo red adsorption – Linearised Langmuir and Freundlich fitting

Linearised Langmuir model: $\frac{C_e}{q_e} = \frac{1}{K_L Q_{max}} + \frac{C_e}{Q_{max}}$

Linearised Freundlich model: $\log q_e = \frac{1}{n} \log C_e + \log K_F$

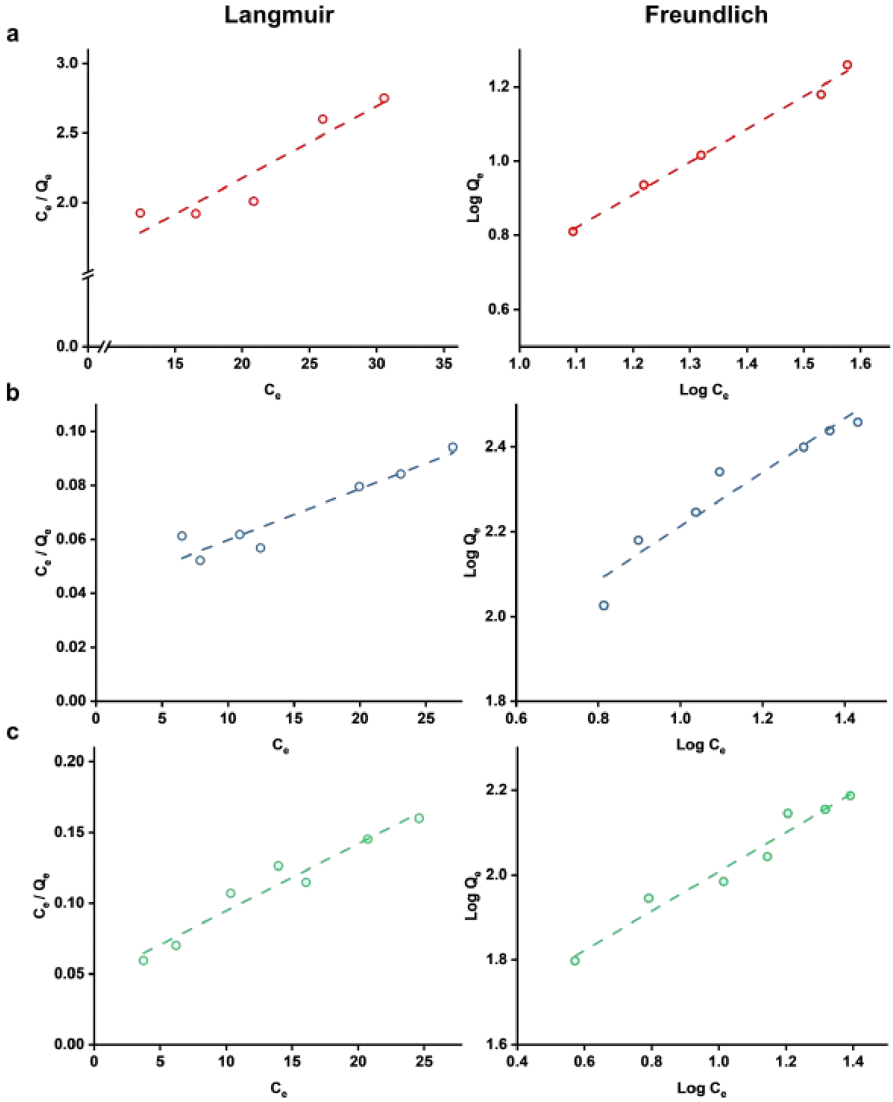

Figure S4 Linearised Langmuir and Freundlich fitting of (a) BC, (b) ZIF-67 and (c) ZIF-BC.

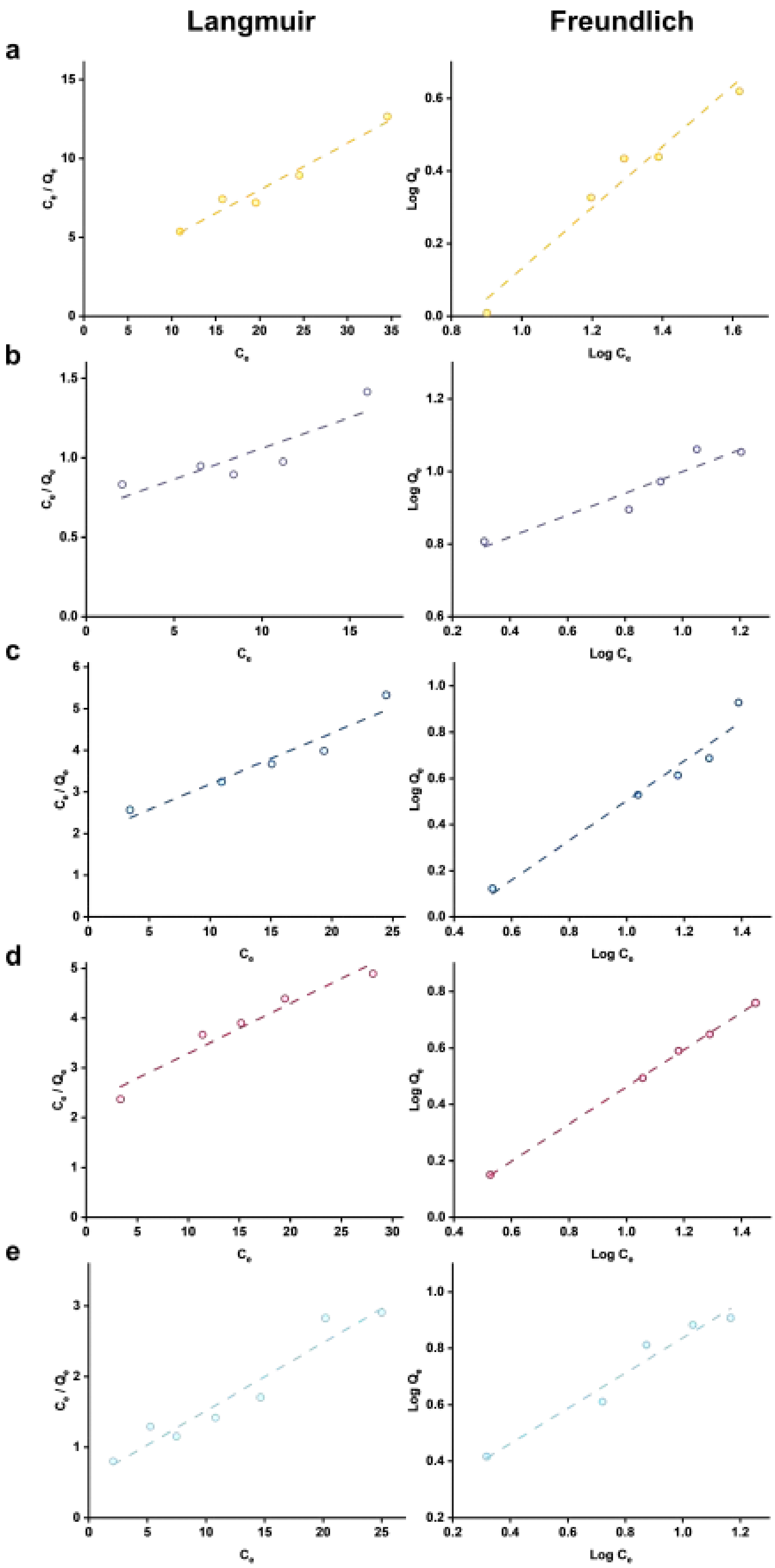

Figure S5 Linearised Langmuir and Freundlich fitting of (a) uncoated woven fabric, (b) ZIF-cotton, (c) 0.25 g m^{-2}, (d) 0.5 g m^{-2} and (e) 1 g m^{-2} ZIF-BC coated woven fabric.

References

1. A. Santmarti, J. W. Teh and K.-Y. Lee, Transparent Poly(methyl methacrylate) Composites Based on Bacterial Cellulose Nanofiber Networks with Improved Fracture Resistance and Impact Strength, *ACS Omega*, 2019, **4**, 9896-9903.
2. W. Sun, X. Zhai and L. Zhao, Synthesis of ZIF-8 and ZIF-67 nanocrystals with well-controllable size distribution through reverse microemulsions, *Chemical Engineering Journal*, 2016, **289**, 59-64.
3. S. A. Han, J. Lee, K. Shim, J. Lin, M. Shahabuddin, J.-W. Lee, S.-W. Kim, M.-S. Park and J. H. Kim, Strategically Designed Zeolitic Imidazolate Frameworks for Controlling the Degree of Graphitization, *Bulletin of the Chemical Society of Japan*, 2018, **91**, 1474-1480.
4. J. Li, T. Tammelin, C. Stone, M. Dennis and K.-Y. Lee, Ultra-Low Grammage Nanocellulose-Coated Woven Fabric with Improved Aerosol Particulate Filtration Performance, *Advanced Materials Interfaces*, 2024, **n/a**, 2400424.
5. A. Santmartí and K. Lee, Chapter 5: crystallinity and thermal, *Nanocellulose and sustainability: production, properties, applications, and case studies. CRC Press, Boca Raton*, 2018, **67**.
6. H. Liu, Z. Guo, Q. Zhang, B. Jin and R. Peng, Zeolite Imidazolate Frameworks-67 Precursor to Fabricate a Highly Active Cobalt-Embedded N-Doped Porous Graphitized Carbon Catalyst for the Thermal Decomposition of Ammonium Perchlorate, *ACS Omega*, 2021, **6**, 25440-25446.
7. M. Wada, J. Sugiyama and T. Okano, Native celluloses on the basis of two crystalline phase (Iα/Iβ) system, *Journal of Applied Polymer Science*, 1993, **49**, 1491-1496.
8. S. Saeed, R. Bashir, S. U. Rehman, M. T. Nazir, Z. A. ALOthman, A. Muteb Aljuwayid, A. Abid and A. Adnan, Synthesis and Characterization of ZIF-67 Mixed Matrix Nanobiocatalysis for CO2 Adsorption Performance, *Frontiers in Bioengineering and Biotechnology*, 2022, **10**.
9. P. Wang, J. Liu, H. Zhan, T. Zhou, Z. Wang and B. Fu, Zeolitic imidazolate framework-67 enabled cellulosic paper for efficient particulate matter capture, *Separation and Purification Technology*, 2024, **333**, 125871.
10. S. Zhang, M. Zhao, H. Li, C. Hou and M. Du, Facile in situ synthesis of ZIF-67/cellulose hybrid membrane for activating peroxymonosulfate to degrade organic contaminants, *Cellulose*, 2021, **28**, 3585-3598.
11. H. S. Jhinjer, A. Singh, S. Bhattacharya, M. Jassal and A. K. Agrawal, Metal-organic frameworks functionalized smart textiles for adsorptive removal of hazardous aromatic pollutants from ambient air, *Journal of Hazardous Materials*, 2021, **411**, 125056.
12. E. Ratna, E. Pramita, S. Eko, S. Dety Oktavia and N. Muhammad, in *Mesoporous Materials*, ed. K. Manjunath, IntechOpen, Rijeka, 2019, DOI: 10.5772/intechopen.84691, p. Ch. 3.
13. D. Liu, P. Jiang, X. Xu, J. Wu, Y. Lu, X. Wang, X. Wang and W. Liu, MOFs decorated sugarcane catalytic filter for water purification, *Chemical Engineering Journal*, 2022, **431**, 133992.
14. T. Kondo and C. Sawatari, A Fourier transform infra-red spectroscopic analysis of the character of hydrogen bonds in amorphous cellulose, *Polymer*, 1996, **37**, 393-399.
15. L. M. Ilharco, A. R. Garcia, J. Lopes da Silva and L. F. Vieira Ferreira, Infrared Approach to the Study of Adsorption on Cellulose: Influence of Cellulose Crystallinity on the Adsorption of Benzophenone, *Langmuir*, 1997, **13**, 4126-4132.

16. S. H. D. Hulleman, J. M. van Hazendonk and J. E. G. van Dam, Determination of crystallinity in native cellulose from higher plants with diffuse reflectance Fourier transform infrared spectroscopy, *Carbohydrate Research*, 1994, **261**, 163-172.
17. Q. Huang, C. Zhao and X. Li, Enhanced electrolyte retention capability of separator for lithium-ion battery constructed by decorating ZIF-67 on bacterial cellulose nanofiber, *Cellulose*, 2021, **28**, 3097-3112.
18. S. Soares, G. Camino and S. Levchik, Comparative study of the thermal decomposition of pure cellulose and pulp paper, *Polymer Degradation and Stability*, 1995, **49**, 275-283.